Biosensors and Bioelectronics 83 (2016) 39–44

Contents lists available at ScienceDirect

Biosensors and Bioelectronics

journal homepage: www.elsevier.com/locate/bios

Ultrasensitive electrochemical detection of protein tyrosine kinase-7 by gold nanoparticles and methylene blue assisted signal amplification

Xiangmin Miao *,[1], Zongbing Li [1], Aihua Zhu, Zhaozhong Feng, Jun Tian, Xue Peng

School of Life Science, Jiangsu Normal University, Xuzhou 221116, PR China

ARTICLE INFO

Article history:
Received 5 March 2016
Received in revised form
9 April 2016
Accepted 12 April 2016
Available online 13 April 2016

Keywords:
Electrochemical aptasensor
Protein tyrosine kinase-7
Positively charged gold nanoparticles
Nafion
DNA modified AuNPs probes
Methylene blue

ABSTRACT

We present here an ultrasensitive and simple strategy for protein tyrosine kinase-7 (PTK7) detection based on the recognition-induced structure change of sgc8 aptamer, and the signal change of methylene blue (MB) that interacted with sandwiched DNA complex. To construct such a sensor, an homogeneous nano-surface was formed firstly on the glass carbon electrode (GCE) by using negatively charged Nafion (Nf) as the inner layer and positively charged gold nanoparticles ((+)AuNPs) as the outer layer, followed by the immobilization of sgc8 aptamer based on Au–S bond. In the presence of helper probe (HP), sandwiched DNA complex was formed between the sgc8 aptamer and the DNA modified gold nanoparticle probe (DNA-AuNPs). Then, a strong current signal was produced due to the capture of abundant MB molecules by both the sandwiched DNA complex and the multiple DNAs that modified on AuNPs surface. However, the specific binding of sgc8 aptamer with PNK7 would trigger a structure transition of it, and directly prevented the following formation of sandwiched structure and the capture of MB. Thus, PTK7 detection could be realized based on monitoring the signal reduction of MB upon incubation of sgc8 aptamer with PTK7. Under optimal conditions, a low detection limit of 372 fM was obtained for PNK7 detection. Due to the employment of sgc8 aptamer, the proposed biosensor exhibited high selectivity to PNK7. Moreover, satisfactory results were obtained when the proposed method was applied for PNK7 detection in cellular debris.

1. Introduction

Protein tyrosine kinase-7 (PKT7), as one type of cell membrane protein, is directly associated with human diseases such as acute myeloid leukemia (AML), colon cancer, gastric cancer, lung cancer and so on (Endoh et al., 2004; Gorringe et al., 2005; Kampen et al., 2011; Shangguan et al., 2008). PTK7 also plays vital roles in numerous physiological functions including molecular recognition, energy transduction and ion regulation (Arinaminpathy et al., 2009; Grimm et al., 2011). Thus, developing novel, sensitive and effective strategies for PKT7 detection is of great importance in clinical diagnosis.

Aptamers are oligonucleotide (DNA or RNA) receptors that obtained in vitro by an evolution process named systematic evolution of ligands by exponential enrichment (SE-LEX) from larger and om-sequence nucleic acid libraries (Ellington et al., 1990; Tuerk et al., 1990). Such aptamers are highly specific to the corresponding targets, and they possess the merits such as easy preparation, thermal stability, reusability and so on. Due to the properties of these aptamers, a number of aptamer-based biosensors have been developed for the quantification of proteins coupling with colorimetric (Su et al., 2013; Wang et al., 2015; Zheng et al., 2014), fluorescent (Feng et al., 2013; He et al., 2012; Wei et al., 2015) and electrochemical (Gui et al., 2014; Jiang et al., 2015; Yu et al., 2015; Zhuang et al., 2014) strategies. Among these biosensors, electrochemical aptasensors have attracted increased research interest because of the merits of them including low cost, easy operation, high sensitivity and good selectivity.

Due to the large surface area and excellent biocompatibility, gold nanoparticles (AuNPs) have been shown to be an excellent candidate for the preparation of biosensors. Thereinto, in electrochemical strategies, AuNPs are mainly utilized for the modification of DNA (Cui et al., 2015; Dong et al., 2012; Wang et al., 2014) and the immobilization of protein (Liu et al., 2014 and Xu et al., 2012), or used to improve the sensitivity of the biosensors due to the high conductivity of them (Li et al., 2015a, 2015a, 2015b; Wang et al., 2013). Methylene blue (MB), as one type of the redox indicators, can interacts with proteins and lipids, and also has high interact capability with single-stranded DNA (ssDNA) that contained high GC contents or double-stranded DNA (dsDNA) based on electrostatic adsorption, such properties of MB allow the great

* Corresponding author.
E-mail address: mxm0107@jsnu.edu.cn (X. Miao).
[1] These authors contributed equally to this work.

http://dx.doi.org/10.1016/j.bios.2016.04.032
0956-5663/

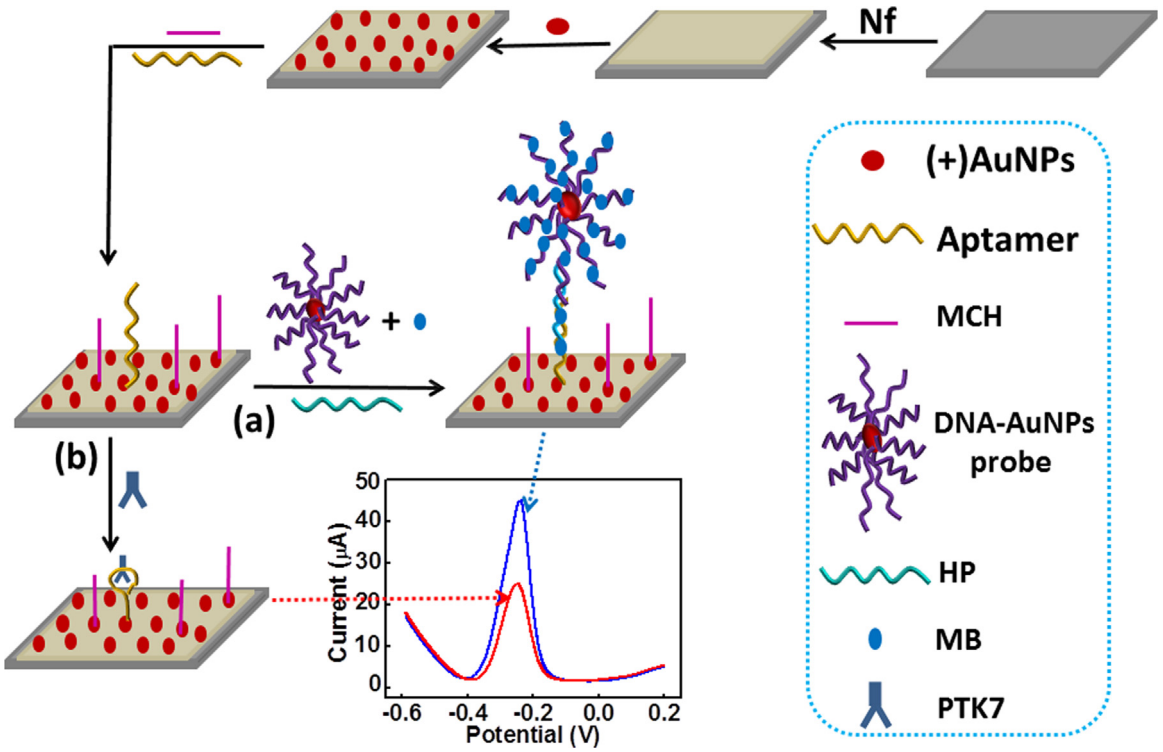

Fig. 1. The scheme of PTK7 detection based on the signal change of MB.

application of it as an excellent redox indicator in electrochemical biosensors preparation (Chen et al., 2008; Li et al., 2015b; Kong et al., 2014; Rohs et al., 2000; Tuite et al., 1994).

To expand the application of MB for biomolecules detection, we reported here an ultrasensitive and simple electrochemical sensor for PTK7 detection based on monitoring the signal change of MB before and after the incubation of sgc8 aptamer with PTK7. As shown in Fig. 1, an homogeneous nano-surface was formed firstly on the glass carbon electrode (GCE) by using negatively charged Nafion (Nf) as the inner layer and about 4 nm of positively charged gold nanoparticles ((+)AuNPs) as the outer layer to enlarge the electrode surface for more aptamer immobilization. Then, numerous sgc8 aptamer strands were effectively immobilized onto above mentioned nano-surface based on Au–S bond. Subsequently, sandwiched DNA complex was formed between the sgc8 aptamer and DNA modified gold nanoparticle probe (DNA-AuNPs) in the presence of helper probe (HP), and a strong current signal of MB was obtained due to the capture of abundant MB on such sandwiched DNA complex. However, the specific binding of PTK7 with sgc8 aptamer in advance would trigger the structure change of sgc8 aptamer, accordingly prevented the following formation of sandwiched structure and the capture of MB. Thus, PTK7 detection could be realized based on monitoring the current signal change of MB oxidation peak by using differential pulse voltammetry (DPV) experiments. Here, about 4 nm of (+)AuNPs with high conductivity and large surface area, was utilized to immobilize the sgc8 aptamer for the first time, which can greatly enhance the amount of aptamer that immobilized on GCE surface, and accordingly in favor of the formation of more sandwiched DNA complex that used for MB capture. In addition, the introduction of (+)AuNPs made the nano-surface positively charged, which would has an electrostatic repulsion to positively charged MB, and accordingly minimized the undesired adsorption of MB on the GCE surface. Thus, the use of (+)AuNPs could effectively improve the accuracy of the sensor for PTK7 detection. Moreover, the proposed method was highly specific for PTK7 detection because of the application of sgc8 aptamer.

2. Experimental section

2.1. Preparation of (+)AuNPs and DNA-AuNPs probes

(+)AuNPs were prepared according to our previous method based on the reduction of 15 mL of $HAuCl_4$ (1.0 mM) using 2 mL of $NaBH_4$ (100 mM) in the presence of 2 mL of CTAB (10 mM) (Li et al., 2015b). The sizes of such (+)AuNPs characterized by TEM (Fig. 2A) and HRTEM (Fig. 2B) were about 4 nm. Another type of AuNPs (16 nm) that used for the preparation of DNA-AuNPs probes and the DNA-AuNPs probes were prepared according to our previous method (Miao et al., 2011).

2.2. Fabrication of DNA-AuNPs/aptamer/(+)AuNPs/Nf modified electrode

Before modification, the glass carbon electrodes (GCE, φ=3 mm, CHI) were polished with 1.0, 0.3, 0.05 μm alumina slurry continuously, and then rinsed with deionized water and sonicated in an ethanol/water bath for 5 min. Then, 5 μL of 1.0 wt% Nf was dipped onto the GCE surface. Subsequently, the Nf/GCE was immersed into (+)AuNPs solution (10.6 nM) and incubated for 90 min at room temperature (RT). After rinsing with deionized water to remove the excess and unreacted regent, the modified electrodes were incubated in aptamer solution over night at RT. Then, the aptamer/(+)AuNPs/Nf/GCE was immersed in 2.0 mM of MCH for 1.5 h to reduce the nonspecific DNA adsorption and to optimize the orientation of the aptamer. At last, the sandwiched DNA complex was obtained on the GCE surface based on the incubation of aptamer/(+)AuNPs/Nf/GCE with DNA-AuNPs solution for 1 h in the presence of helper probe (HP). Before using, the modified electrodes were kept at 4 °C.

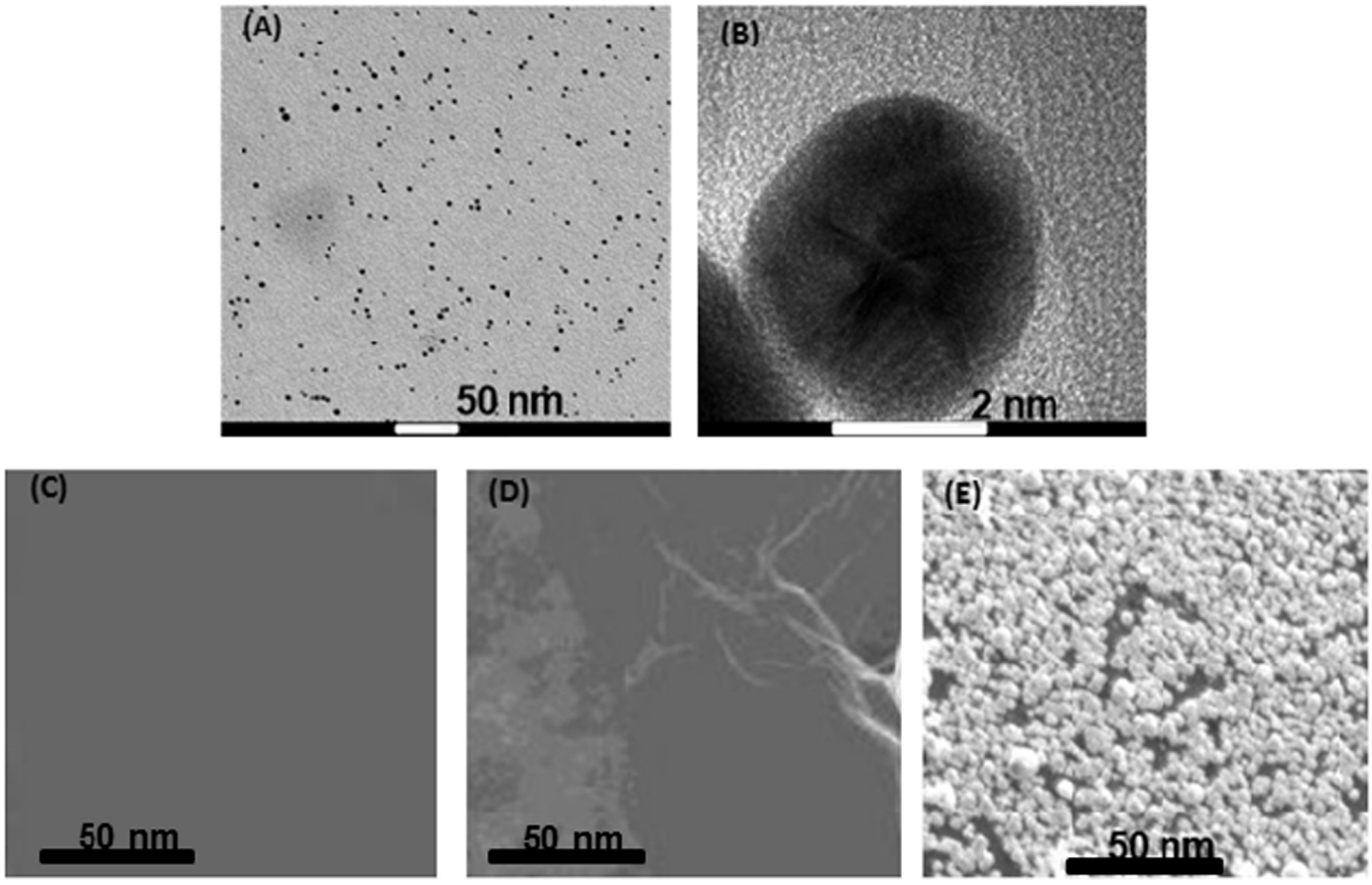

Fig. 2. (A) TEM images of (+)AuNPs; (B) HRTEM images of (+)AuNPs; SEM images of bare GEC (C), Nf/GCE (D) and (+)AuNPs/Nf/GCE (E).

2.3. Electrochemical detection of PTK7

To construct electrochemical PTK7 detection, aptamer/(+)AuNPs/Nf/GCE was immersed into Tris-buffer (50 mM, pH 7.4) that contained different concentration of PTK7 for 50 min at 37 °C. Subsequently, above modified electrodes were immersed into DNA-AuNPs solution (3.0 μM) for 1 h in the presence of HP to form DNA-AuNPs/aptamer/(+)AuNPs/Nf/GCE. Then, the DNA-AuNPs/aptamer/(+)AuNPs/Nf/GCE were immersed into the solution that containing 50 μM of MB for 30 min to realize the capture of different amount of MB (after each step of modification, the electrode was rinsed with Tris-buffer thoroughly). At last, the electrochemical characteristics of the resulting sensor were investigated in 50 mM of Tris-buffer (pH 7.4) by using differential pulse voltammetry (DPV) experiments from −0.6 to 0.2 V.

3. Results and discussion

3.1. SEM images of different GCE surfaces

To prove the formation of (+)AuNPs nano-surface, SEM images were shown in Fig. 2, an uniform and smooth surface was obtained for bare GCE (Fig. 2C) while an obvious thin film was formed on the GCE surface after 5 μL of 1.0 wt% Nf was dipped onto the GCE surface and dried in the air (Fig. 2D). Then, after the effective adsorption of (+)AuNPs, we could observe that numerous (+)AuNPs were well-distributed on the Nf surface (Fig. 2E).

3.2. Electrochemical behavior of MB

To confirm the feasibility of the sensor, the electrochemical property of MB at (+)AuNPs/Nf/GCE was investigated by using DPV experiments. As shown in Fig. 3A, an obvious oxidation peak of MB at about −0.25 V was observed when the (+)AuNPs/Nf/GCE was scanned in Tris-buffer (50 mM, pH 7.4) that contained 50 μM of MB, and the current intensity of (+)AuNPs/Nf/GCE (curve b) was greater than that of the bare GCE (curve a). Such results illustrated that (+)AuNPs/Nf/GCE can facilitates the electron-transfer of MB, accordingly improving the electrochemical performances of the sensor.

In this work, PTK7 detection was completed based on monitoring the electrochemical signal change of MB oxidation peak before and after the specific binding of aptamer with PTK7. Thus, the undesired adsorption of MB on the electrode surface would affect the detection of PTK7. To eliminate such possibility, the Nf/GCE and (+)AuNPs/Nf/GCE were immersed into Tris-buffer (50 mM, pH 7.4) that contained 50 μM of MB, and incubated for 30 min. After that, the electrodes were rinsed with Tris-buffer for three times, followed by constructing DPV experiments. As seen in Fig. 3B, a large oxidation peak of MB was obtained at Nf/GCE (curve a), while that for the (+)AuNPs/Nf/GCE was weak and even could be neglected (curve b). This might be due to that Nf used in this work is negatively charged, which can effectively adsorb the positively charged MB onto its surface, accordingly generated strong current signal of MB. However, the self-assembly of (+)AuNPs would make the electrode surface positively charged, resulting in the electrostatic repulsion between (+)AuNPs and MB. Thus, the introduction of (+)AuNPs can greatly decrease the undesired adsorption of MB on the electrode surface and enhance the

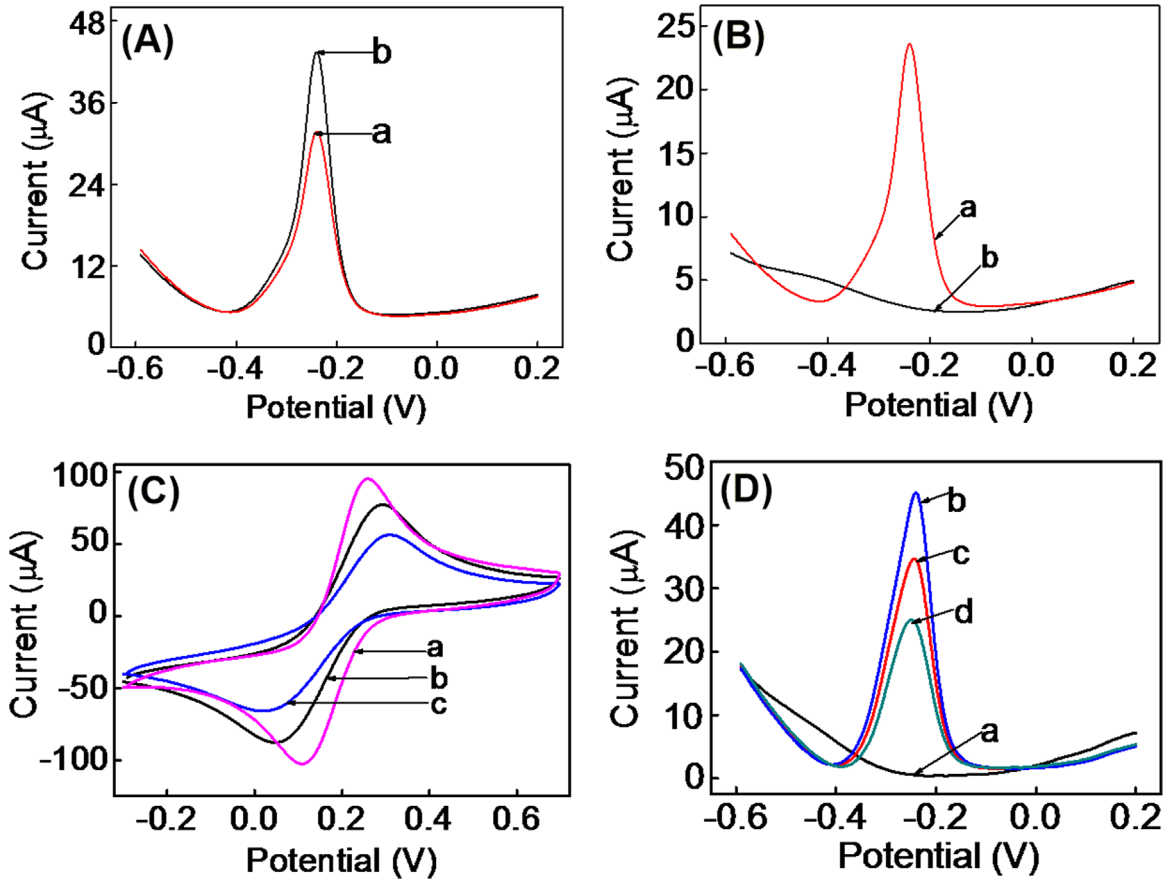

Fig. 3. (A) DPV curves of the GCE (a) and (+)AuNPs/Nf/GCE (b) in Tris-buffer (50 mM, pH 7.4) that contained 50 μM of MB; (B) DPV curves of the Nf/GCE (a) and (+)AuNPs/Nf/GCE (b) in Tris-buffer (50 mM, pH 7.4) after the two modified electrodes were incubated in 50 μM of MB; (C) CV curves obtained in 5 mM of $[Fe(CN)_6]^{3-/4-}$ of (+)AuNPs/Nf/GCE (a), aptamer/(+)AuNPs/Nf/GCE (b) and DNA-AuNPs/aptamer/(+)AuNPs/Nf/GCE (c); (D) DPV curves obtained in Tris-buffer (50 mM, pH 7.4) of the GCE (a), DNA-AuNPs/aptamer/(+)AuNPs/Nf/GCE (b) and DNA-AuNPs/aptamer/(+)AuNPs/Nf/GCE in the presence of 50 (c) and 300 pM (d) of PTK7 separately.

accuracy of the sensor for PTK7 detection.

3.3. Characterization of the sensor

To further prove the effective formation of sandwiched DNA complex, different modified electrodes were investigated in 5 mM of $[Fe(CN)_6]^{3-/4-}$. As shown in Fig. 3C, an obvious redox peak of $[Fe(CN)_6]^{3-/4-}$ was observed on the (+)AuNPs/Nf/GCE (curve a), due to the good conductivity of (+)AuNPs. However, after the immobilization of sgc8 aptamer onto the (+)AuNPs nano-surface, an obvious decrease of the redox peak of $[Fe(CN)_6]^{3-/4-}$ was observed (curve b), because of the fact that the sgc8 aptamer is negatively charged, which can produce electrostatic repulsion to negatively charged $[Fe(CN)_6]^{3-/4-}$ and hinder the electron transfer between the electrode and $[Fe(CN)_6]^{3-/4-}$. Then, after the formation of sandwiched DNA complex, the current signal of $[Fe(CN)_6]^{3-/4-}$ redox peak decreased further (curve c), which proved the effective formation of sandwiched DNA complex and enhanced the negative charge of electrode surface.

The electrochemical detection of PTK7 was performed based on observing the electrochemical signal change of MB before and after the specific binding of sgc8 aptamer with PTK7. Fig. 3D showed that a strong oxidation peak of MB was obtained after the MB/DNA-AuNPs/aptamer/(+)AuNPs/Nf/GCE was scanned in blank Tris-buffer using DPV (curve b) compared to the bare GCE (curve a). However, upon incubation of aptamer/(+)AuNPs/Nf/GCE with 50 and 300 pM of PTK7 in advance, specific binding between aptamer and PTK7 would happen, resulting in the structure change of sgc8 aptamer, which would directly hinder the formation of sandwiched DNA complex and the capture of MB, and therefore, the current signal of MB oxidation peak was gradually decreased along with the increase of PTK7 concentration (curve c and d).

3.4. Optimization of experimental conditions

In this article, Nf was used for the self-assembly of (+)AuNPs. Hence, the coated amount of Nf on the GCE surface would directly affect the self-assembly of (+)AuNPs, accordingly affected the properties of the sensor. As seen from Fig. S1A, an optimal peak current was obtained when 5 μL of 1.0 wt% Nf was coated onto the electrode surface for (+)AuNPs self-assembly. Therefore, 1.0 wt% of Nf was used for the preparation of Nf film on the electrode surface.

Adsorption of (+)AuNPs used for sgc8 aptamer immobilization is an important factor that can affect the properties of the sensor. Fig. S1B showed the time effect of (+)AuNPs adsorption on the oxidation peak current of MB, and the peak current initially increased along with the increase of (+)AuNPs adsorption time in the range of 10–90 min, and then reached a plateau after 90 min. Such results illustrated that the adsorption of (+)AuNPs could be realized within 90 min. Thus, 90 min was selected in this work.

The capture time of MB could directly affect the amount of MB that interacted with sgc8 aptamer. As shown in Fig. S1C, the increase of MB capture time from 5 to 30 min would result in increasing current signal of the sensor, and 30 min of the capture time produce the largest current signal, indicating that the amount of MB that interacted with sgc8 aptamer was proportional to the capture time. Considering the sensitivity of the sensor, 30 min was

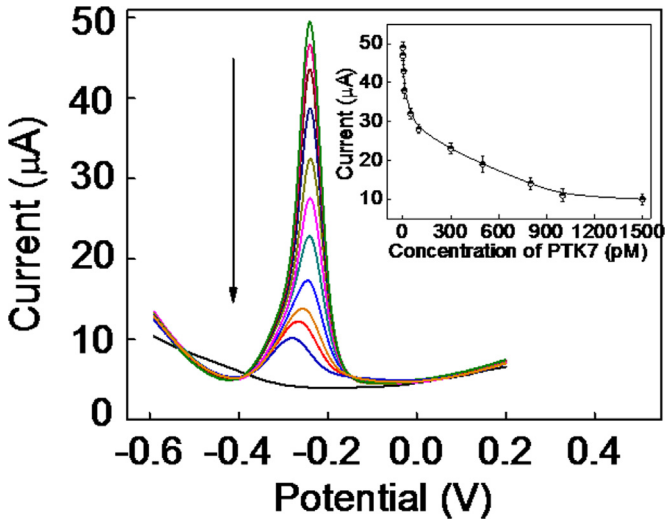

Fig. 4. The DPV curves of PTK7 detection in 50 mM of Tris-buffer (pH 7.4) by using the proposed method (Inset: calibration curve for PTK7 detection).

utilized for the capture of MB. In addition, the electrochemical signal change of MB was mainly based on the specific binding of PTK7 with sgc8 aptamer. Thus, the effect of binding time between PTK7 and sgc8 aptamer was also evaluated in Fig. S1D, and the current change (ΔI) before and after PTK7 binding increased with the increasing binding time in the range of 10–50 min. Thus, 50 min was chosen as the optimal binding time.

3.5. Characteristics of the sensor for PTK7 detection

Under optimal conditions, quantitative detection of PTK7 was carried out by incubating aptamer/(+)AuNPs/Nf/GCE in Tris-buffer that contained different concentration of PTK7, followed by the incubation with DNA-AuNPs probes for 1 h and further incubation with MB solution for 30 min. After rinsing with Tris-buffer, the resulted sensor was then measured in Tris-buffer by using DPV experiments. As shown in Fig. 4, the oxidation peak currents decreased along with the increase of PTK7 concentration, and two linear ranges between the peak currents and the PTK7 concentration was obtained from 1.0 pM to 100 pM and from 100 pM to 1.0 nM. The regression equation formed was I=49.74–0.30c (pM) and I=29.05–0.02c (pM), with corresponding correlation coefficients of 0.991 and 0.996. The detection limit of the proposed method is 372 fM, which is lower than other electrochemical-based methods (Erdem et al., 2000; Erdem et al., 2014; Fang et al., 2016) because of the amplification of (+)AuNPs. Moreover, MB indicator used in this work can self-interact with DNA strands, without needing any chemical or biological labeling, leading to the sensor gradually simple to operate.

3.6. Selectivity and reproducibility of the sensor

The selectivity of the sensor was evaluated by incubating the aptamer/(+)AuNPs/Nf/GCE with PTK7 and three other non-specific proteins including Immunoglobulin G (IgG), Immunoglobulin A (IgA), human serum albumin (HSA) and human plasma fibronectin (Fn), respectively. From the results in Fig. S2A, it could be seen that the current change (ΔI) of MB for IgG, IgA, HSA and Fn was very little in contrast to that for PTK7. Such results proved that the proposed method for PTK7 detection is highly specific.

Meantime, the reproducibility of the sensor was examined by detecting 200 pM of PTK7 for 15 times using the same immunosensor, and a relative standard deviation (RSD) of 7.3% was obtained, which indicated the acceptable reproducibility of the sensor.

3.7. PTK7 assay in cellular debris and real patient samples

To evaluate the application of the proposed method, the performance of the sensing platform was investigated for PTK7 in the presence of cellular debris obtained from malignant melanoma A375 cells, which shows reduced expression of PTK7 (Easty et al., 1997). Based on monitoring the proposed sensor in a reaction system that contained 0.5% (v/v) cell extract, the electrochemical signal of MB increased along with the increase of PTK7 concentration (Fig. S2B). Such results demonstrated that this assay could be potentially applied for the detection of PTK7 in biological samples. Moreover, ten protein extracted samples of lung cancer patients were obtained from The First People's Hospital of Xuzhou and stored at −80 °C, and the accuracy of PTK7 detection using our method was evaluated by comparing the results from enzyme-linked immunosorbent based assay (ELISA) (Fig. S2C). The regression equation of the concentration of PTK7 obtained from our platform(x) and ELISA technique was y=0.938x+0.452, with a coefficient of 0.996, indicating a potential application of our method in protein detection of real samples.

4. Conclusion

In conclusion, an ultrasensitive electrochemical aptasensor was developed for PTK7 detection. Under optimal conditions, a low detection limit of 372 fM was obtained because of that the application of (+)AuNPs nanoscale surface can greatly enhance the amount of sgc8 aptamer that immobilized on the electrode, and accordingly in favor of the formation of more sandwiched DNA complex that used for MB capture. Meantime, the using of (+)AuNPs nanoscale surface greatly eliminated the undesirable adsorption of MB on the electrode surface and largely improved the accuracy of the sensor. Moreover, the proposed method is highly specific for PTK7 detection because of the application of sgc8 aptamer, and satisfactory results were obtained for PTK7 detection in cellular debris.

Acknowledgements

This work was supported by the National Natural Science Foundation of China (21305053) and the Natural Science Fund in Jiangsu Province (BK20130227).

Appendix A. Supporting information

Supplementary data associated with this article can be found in the online version at http://dx.doi.org/10.1016/j.bios.2016.04.032.

References

Arinaminpathy, Y., Khurana, E., Engelman, D.M., Gerstein, M.B., 2009. Drug Discov. Today 14, 1130–1135.
Cui, H.F., Xu, T.B., Sun, Y.L., Zhou, A.W., Cui, Y.H., Liu, W., Luong, J.H.T., 2015. Anal. Chem. 87, 1358–1365.
Chen, J., Zhang, J., Wang, K., Lin, X., Huang, L., Chen, G., 2008. Anal. Chem. 80, 8028–8034.
Dong, H.F., Zhu, Z., Ju, H.X., Yan, F., 2012. Biosens. Bioelectron. 33, 228–232.
Endoh, H., Tomida, S., Yatabe, Y., Konishi, H., Osada, H., Tajima, K., Kuwano, H., Takahashi, T., Mitsudomi, T., 2004. J. Clin. Oncol. 22, 811–819.
Easty, D.J., Mitchell, P.J., Patel, K., Florenes, V.A., Spritz, R.A., Bennett, D.C., 1997. Int. J. Cancer 71, 1061–1065.
Ellington, A.D., Szostak, J.W., 1990. Nature 346, 818–822.
Erdem, A., Kerman, K., Meric, B., Akarca, U.S., Ozsoz, M., 2000. Anal. Chim. Acta 422, 139–149.
Erdem, A., Eksin, E., Muti, M., 2014. Colloid Surf. B 115, 205–211.

Fang, S.M., Dong, X.D., Ji, H.F., Liu, S.L., Yan, F.F., Peng, D.L., He, L.H., Wang, M.H., Zhang, Z.H., 2016. Microchim. Acta 183, 633–642.
Feng, T.T., Ma, H.M., 2013. Analyst 138, 2438–2442.
Gorringe, K.L., Boussioutas, A., Bowtell, D.D.L., 2005. Genes Chromosom. Cancer 42, 247–259.
Gui, G.F., Zhuo, Y., Chai, Y.Q., Xiang, Y., Yuan, R., 2014. Anal. Chem. 86, 5873–5880.
Grimm, D., Bauer, J., Pietsch, J., Infanger, M., Eucker, J., Eilles, C., Schoenberger, J., 2011. Curr. Med. Chem. 18, 176–190.
He, Y., Lin, Y., Tang, H.W., Pang, D.W., 2012. Nanoscale 4, 2054–2059.
Jiang, B.Y., Li, F.Z., Yang, C.Y., Xie, J.Q., Xiang, Y., Yuan, R., 2015. Anal. Chem. 87, 3094–3098.
Kampen, K.R., 2011. J. Membr. Biol. 242, 69–74.
Kong, R.M., Song, Z.L., Meng, H.M., Zhang, X.B., Shen, G.L., Yu, R.Q., 2014. Biosens. Bioelectron. 54, 442–447.
Liu, X., Li, W.J., Li, L., Yang, Y., Mao, L.G., Peng, Z., 2014. Sens. Actuators B: Chem. 191, 408–414.
Li, F.Y., Han, J., Jiang, L.P., Wang, Y.L., Li, Y.Y., Dong, Y.H., Wei, Q., 2015a. Biosens. Bioelectron. 68, 626–632.
Li, Z.B., Miao, X.M., Xing, K., Zhu, A.H., Ling, L.S., 2015a. Biosens. Bioelectron. 74, 687–690.
Li, Z.B., Miao, X.M., Zhu, A.H., Ling, L.S., 2015b. Biochem. Eng. J. 103, 205–210.
Li, F.Y., Peng, J., Zheng, Q., Guo, X., Tang, H., Yao, S.Y., 2015b. Anal. Chem. 87, 4806–4813.
Miao, X.M., Xiong, C., Wang, W.W., Ling, L.S., 2011. Chem. Eur. J. 17, 11230–11236.
Rohs, R., Sklenar, H., Lavery, R., Röder, B., 2000. J. Am. Chem. Soc. 122, 2860–2866.
Shangguan, D., Cao, Z., Meng, L., Mallikaratchy, P., Sefah, K., Wang, H., Li, Y., Tan, W., 2008. J. Proteome Res. 7, 2133–2139.
Su, J., Zhou, W.J., Xiang, Y., Yuan, R., Chai, Y.Q., 2013. Chem. Commun. 49, 7659–7661.
Tuerk, C., Gold, L., 1990. Science 249, 505–510.
Tuite, E., Norden, B., 1994. J. Am. Chem. Soc. 116, 1548–7556.
Wang, C.K., Dong, X.Y., Liu, Q., Wang, K., 2015. Anal. Chim. Acta 860, 83–88.
Wang, Z.H., Sun, N., He, Y., Liu, Y., Li, J.H., 2014. Anal. Chem. 86, 6153–6159.
Wei, Y., Zhang, J., Wang, X., Duan, Y.X., 2015. Biosens. Bioelectron. 65, 16–22.
Wang, G.F., Gang, X., Zhou, X., Zhang, G., Huang, H., Zhang, X.J., Wang, L., 2013. Talanta 103, 75–80.
Xu, Q.N., Yan, F., Lei, J.P., Leng, C., Ju, H.X., 2012. Chem. Eur. J. 18, 4994–4998.
Yu, P., He, X.L., Zhang, L., Mao, L.Q., 2015. Anal. Chem. 87, 1373–1380.
Zheng, C., Zheng, A.X., Liu, B., Zhang, X.L., He, Y., Li, J., Yang, H.H., Chen, G.N., 2014. Chem. Commun. 50, 13103–13106.
Zhuang, J.Y., He, Y., Chen, G.N., Tang, D.P., 2014. Electrochem. Commun. 47, 25–28.